

The phase diagram of the Polyakov Nambu Jona-Lasinio approach for finite chemical potentials

D. Fuseau¹, T. Steinert² and J. Aichelin^{1,3}

¹ *SUBATECH, University of Nantes, IMT Atlantique,
IN2P3/CNRS 4 rue Alfred Kastler, 44307 Nantes cedex 3, France*

² *Institut für Theoretische Physik, Heinrich Buff Ring 16, 35392 Giessen, Germany and*
³ *Frankfurt Institute for Advanced Studies, Ruth Moufang Str. 1, 60438 Frankfurt, Germany*

(Dated: December 21, 2024)

We extend the SU(3) (Polyakov) Nambu Jona-Lasinio in two ways: We introduce the next to leading order contribution (in N_c) in the partition function. This contribution contains explicit mesonic terms. We introduce a coupling between the gluon field and the quark degrees of freedom which goes beyond a simple rescaling of the critical temperature. With both these improvements we can reproduce, for vanishing chemical potentials, the lattice results for the thermal properties of a strongly interacting system like pressure, energy density, entropy density, interaction measure and the speed of sound. Also the expansion parameter towards small but finite chemical potentials agrees with the lattice results. Extending the calculations to finite chemical potentials (what does not require any new parameter) we find a first order phase transition up to a critical end point of $T_{CEP} = 110 \text{ MeV}$ and $\mu_q = 320 \text{ MeV}$. For very large chemical potentials, we find agreement with pQCD calculations. We calculate the mass of mesons and baryons as a function of temperature and chemical potential and the transition between the hadronic and the chirally restored phase. These calculations provide an equation of state in the whole T, μ plane an essential ingredient for dynamical calculations of ultra-relativistic heavy ion collisions but also for the physics of neutron stars and neutron star collisions.

I. INTRODUCTION

The study of the phase diagram of strongly interacting matter has recently gained a lot of interest. This is on the one side due to the new NICA (Dubna, Russia) and FAIR (Darmstadt, Germany) facilities which are presently under construction. They will allow high precision studies in the region of a large baryon chemical potential, μ , a region of the (T, μ) , T being the temperature) phase diagram which is presently inaccessible. On the other side the new field of simulations of collisions of neutron stars, triggered by the observation of gravitational waves from such events, needs as input this phase diagram for a large range of densities and temperatures [1].

At zero baryochemical potential the thermodynamical quantities of strongly interacting matter have been calculated in lattice gauge calculations which gained over the years in precision and where the results of different groups agree now within the error bars [2, 3]. These results have been compared with experimental results at RHIC (Brookhaven National Laboratory) and LHC (CERN) in a number of ways. This includes the observation that the multiplicity of the observed hadrons can be well described using a statistical model with a very small baryochemical potential and a temperature close to the critical temperature of the lattice calculation, defined as the inflection point of the pressure as a function of the temperature [4–6]. Hydrodynamical calculations or kinetic approaches using the lattice equation of state describe quite well the experimental results of a multitude of hadron observables [7]. Also the experimentally observed fluctuation of conserved quantities has been compared in detail with the results of lattice calcula-

tion [8], although this is quite complicated taking into account the finite size of the system, the finite experimental acceptance and the inelastic hadron collisions after "freeze out", when the mean free path is too long to maintain thermal equilibrium.

Due to the sign problem lattice calculations cannot be extended to finite μ . Methods, like a Taylor expansion [9] or an analytical continuation from imaginary chemical potentials [10], have been developed to extrapolate the thermodynamical quantities away from the $\mu = 0$ line but the deeper one penetrates into the finite μ region the more one enters unknown territory. Being presently outside of the range of lattice gauge calculation this is the realm of phenomenological models and subject of intensive studies. Many of these approaches suggest that the cross over, observed for $\mu = 0$, continues for finite μ , however with a steeper and steeper slope, before it merges finally into a critical end point followed by a first order phase transition for even larger μ [11–13]. At zero temperature and large μ perturbative three-loop QCD calculations are available [14, 15] which allow in this limit to compare phenomenological approaches with QCD.

In this paper we study the phase diagram and the thermal properties of 3 flavour QCD at finite chemical potential in the Polyakov Nambu Jona-Lasinio (PNJL) approach, extending the work of refs. [16, 17]. This model has the merit that it is based on the symmetries of the QCD and that it is conceptually rather simple. Few vacuum observables are sufficient to fix the parameters of the theory, the extension towards finite μ is straight forward and does not need the introduction of new parameters. The PNJL model [18–21] is an improved version of the Nambu Jona-Lasinio model [22]

in which the interaction among quarks is described by a four-point interaction assuming that the gluon mass is large as compared to the momentum transfer between the quarks. Such a mass increase of gluons (and quarks) is indeed observed in nonperturbative QCD calculations. For a review we refer to [23]. Consequently, in NJL gluons do not appear in the quark dynamics. At low temperatures the chiral symmetry of the Lagrangian is spontaneously broken by a chiral condensate and the quarks acquire a quasi particle mass. Mesons emerge as color singlet $q\bar{q}$ modes. A Fierz transformation projects the Lagrangian to various quark-antiquark and di-quark channels. The latter allows to describe baryon masses and to predict their temperature dependence [24]. NJL type models have a long history and have been extensively used to describe the dynamics and thermodynamics of light hadrons and baryons. They offer the possibility to study in a simple way and with a very limited number of parameters, adjusted to vacuum physics, the basic features of low temperature QCD, the basic mechanism for the spontaneous breakdown of chiral symmetry, but suffer from the absence of confinement, a consequence of the replacement of the local $SU(N_c)$ gauge invariance of QCD by a global $SU(N_c)$ symmetry. For more details we refer to the review articles[25–27].

In the PNJL model quarks couple to a static homogeneous Polyakov loop effective potential which is conveniently parametrized by using pure gauge lattice QCD calculation at finite temperatures in addition to the coupling to the chiral condensate. The model reproduced successfully [20] the lattice data from the Bielefeld group [28, 29]. These calculations, however, have been further refined and nowadays all lattice groups agree on the phase diagram at zero baryon chemical potential. With these new results [2, 3] the standard PNJL calculations of ref. [20] do not agree anymore.

One of the advantages of the PNJL model is that it allows for a straight forward calculation of the phase diagram in the whole T, μ plane without introducing any further parameters. To make such calculations useful it is, however, necessary to reproduce the lattice calculation at $\mu = 0$. It is the purpose of this article to show that by including the next to leading order in the large N_c expansion and by redefining the interaction between the Polyakov loop potential and the quarks we obtained a good agreement with the newest lattice equation of state not only at $\mu = 0$ but also for the expansion coefficient of the Taylor expansion toward finite μ .

The paper is organized as follows: we will start by describing the traditional PNJL model in section 2. In section 3, we discuss the difference of our approach as compared to the standard PNJL model. In section 4 we present our results. First we compare our results for $\mu = 0$ with those of lattice gauge calculations, then we present the phase diagram at finite chemical potential and discuss finally the appearance of a first order phase transition for low temperatures and a finite chemical potential. Finally, in section 5, we present our conclusions.

II. PNJL MODEL

A. PNJL Lagrangian and Polyakov loop

The PNJL[18–21, 24] model is an extension of the NJL model taking under consideration thermal gluons on the level of a mean field. The quark-quark interaction remains local, the gluons are only present as a continuous mean field surrounding the quarks. It can be associated to the $\frac{1}{4}F_{\mu\nu}^a F^{a\mu\nu}$ term in the QCD Lagrangian. We consider the Lagrangian of the PNJL model [18–21, 24] with (color neutral) pseudoscalar and scalar interactions (neglecting the vector and axial-vector vertices for simplicity),

$$\begin{aligned} \mathcal{L}_{PNJL} = & \sum_i \bar{\psi}_i (i\not{D} - m_{0i} + \mu_i \gamma_0) \psi_i \\ & + G \sum_a \sum_{ijkl} [(\bar{\psi}_i i\gamma_5 \tau_{ij}^a \psi_j) (\bar{\psi}_k i\gamma_5 \tau_{kl}^a \psi_l) \\ & + (\bar{\psi}_i \tau_{ij}^a \psi_j) (\bar{\psi}_k \tau_{kl}^a \psi_l)] \\ & - H \det_{ij} [\bar{\psi}_i (\mathbb{I} - \gamma_5) \psi_j] - H \det_{ij} [\bar{\psi}_i (\mathbb{I} + \gamma_5) \psi_j] \\ & - \mathcal{U}(T; \Phi, \bar{\Phi}) . \end{aligned} \quad (1)$$

$i, j, k, l = 1, 2, 3$ are the flavor indices and τ^a ($a = 1, \dots, 8$) are the $N_f = 3$ flavor generators with the normalization

$$\text{tr}_f (\tau^a \tau^b) = 2\delta^{ab} , \quad (2)$$

with tr_f denoting the trace in flavor space.

In the Lagrangian (1) the bare quark masses are represented by m_{0i} and their chemical potential by μ_i . The covariant derivative in the Polyakov gauge reads $D^\mu = \partial^\mu - i\delta^{\mu 0} A^0$, with $A^0 = -iA_4$ being the temporal component of the gluon field in Euclidean space (we denote $A^\mu = g_s A_a^\mu T_a$). The coupling constant for the scalar and pseudoscalar interaction G is taken as a free parameter (fixed e.g. by the pion mass in vacuum).

The third term of Eq. (1) is the so-called 't Hooft Lagrangian. It mimics the effect of the axial $U(1)$ anomaly, accounting for the physical splitting between the η and the η' mesons. H is a coupling constant (fixed by the value of $m_{\eta'} - m_\eta$) and \mathbb{I} is the identity matrix in Dirac space.

Finally, $\mathcal{U}(T, \Phi, \bar{\Phi})$ is the so-called Polyakov-loop effective potential used to account for static gluonic contributions to the pressure. The Polyakov line and the Polyakov loop are, respectively, defined as

$$L(\mathbf{x}) = \mathcal{P} \exp \left(i \int_0^{1/T} d\tau A_4(\tau, \mathbf{x}) \right) , \quad \Phi(\mathbf{x}) = \frac{1}{N_c} \text{tr}_c L(\mathbf{x}) , \quad (3)$$

where \mathcal{P} is the path-integral ordering operator, and the trace tr_c is taken in the color space.

Following [20] we take an homogeneous Polyakov loop field $\Phi(\mathbf{x}) = \Phi = \text{const.}$, and calculate the expectation

values $\langle \Phi \rangle(T)$, $\langle \bar{\Phi} \rangle(T)$ that minimize the effective potential $\mathcal{U}(T, \Phi, \bar{\Phi})$ at a given temperature

$$\left. \frac{\partial \mathcal{U}(T, \Phi, \bar{\Phi})}{\partial \Phi} \right|_{\Phi=\langle \Phi \rangle(T), \bar{\Phi}=\langle \bar{\Phi} \rangle(T)} = 0, \quad \left. \frac{\partial \mathcal{U}(T, \Phi, \bar{\Phi})}{\partial \bar{\Phi}} \right|_{\Phi=\langle \Phi \rangle(T), \bar{\Phi}=\langle \bar{\Phi} \rangle(T)} = 0. \quad (4)$$

The value of the potential for the expectation values $\langle \Phi \rangle(T)$, $\langle \bar{\Phi} \rangle(T)$, $\mathcal{U}(T, \langle \Phi \rangle(T), \langle \bar{\Phi} \rangle(T))$, gives up to a minus sign the pressure of the gluons in Yang Mills (YM) theory, corresponding to QCD for infinitely heavy quarks. The comparison with lattice gauge calculations for pure YM serves therefore as a guideline for the parametrization of the effective potential $U(T)$.

$$-P(T) = \mathcal{U}(T, \langle \Phi \rangle(T), \langle \bar{\Phi} \rangle(T)). \quad (5)$$

Different possible parametrisations of the effective potential $U(T, \phi, \bar{\phi})$ have been advanced. We follow here our earlier work and use the "polynomial parametrisation" for the YM effective potential:

$$\frac{U(T, \phi, \bar{\phi})}{T^4} = -\frac{b_2(T)}{2} \bar{\phi}\phi - \frac{b_3}{6} (\bar{\phi}^3 + \phi^3) + \frac{b_4}{4} (\bar{\phi}\phi)^2 \quad (6)$$

with the parameters: $b_2(T) = a_0 + a_1(\frac{T_0}{T}) + a_2(\frac{T_0}{T})^2 + a_3(\frac{T_0}{T})^3$ which are displayed in tab. I.

a_0	a_1	a_2	a_3	b_3	b_4	T_0
6.75	-1.95	2.625	-7.44	0.75	7.5	270 MeV

TABLE I. Table of PNJL parameters for a polynomial parametrisation

T_0 is the critical temperature of a Yang-Mills potential.

B. Thermodynamics in the presence of the effective potential

All thermodynamical quantities can be obtained from the partition function here written in the path integral formalism:

$$Z[\bar{q}, q] = \int \mathcal{D}_{\bar{q}} \mathcal{D}_q \left\{ \int_0^\beta d\tau \int_V d^3x \mathcal{L}_{PNJL} \right\}. \quad (7)$$

After the standard bosonisation procedure, we obtain the mean field expression of the partition function:

$$Z[\bar{q}, q] = \exp \left\{ - \int_0^\beta d\tau \int_V \frac{\sigma_{MF}^2}{4G} + Tr \ln S_{MF}^{-1} \right\}. \quad (8)$$

$\Omega(T, \mu)$, the grand potential, (we suppress here the volume dependence as we work in the infinite matter limit) is related to the partition function by:

$$\Omega = -T \ln(Z). \quad (9)$$

We obtain for the quark part of the PNJL Lagrangian [21, 24] at the order of $(\frac{1}{N_c})^{-1}$.

$$\begin{aligned} & \Omega_q^{(-1)}(T, \mu_i, \langle \bar{\psi}_i \psi_i \rangle, \Phi, \bar{\Phi}) \\ &= \ln(Tr[\exp(-\beta \int dx^3 (-\bar{\psi}(i\cancel{D} - m)\psi - \mu\bar{\psi}\psi)]) \\ &+ 2G \sum_k \langle \bar{\psi}_k \psi_k \rangle^2 - 4K \prod_i \langle \bar{\psi}_k \psi_k \rangle + U_{PNJL} \\ &= 2G \sum_i \langle \bar{\psi}_i \psi_i \rangle^2 - 4H \prod_i \langle \bar{\psi}_i \psi_i \rangle - 2N_c \sum_i \int \frac{d^3k}{(2\pi)^3} E_i \\ &- 2TN_c \sum_i \int \frac{d^3k}{(2\pi)^3} \left[\frac{1}{N_c} \text{tr}_c \log \left(1 + L e^{-(E_i - \mu_i)/T} \right) \right. \\ &\left. + \frac{1}{N_c} \text{tr}_c \log \left(1 + L^\dagger e^{-(E_i + \mu_i)/T} \right) \right], \quad (10) \end{aligned}$$

where $E_i = \sqrt{k^2 + m_i^2}$. Note that $G \sim \mathcal{O}(1/N_c)$, $H \sim \mathcal{O}(1/N_c^2)$ and $\langle \bar{\psi}_i \psi_i \rangle \sim \mathcal{O}(N_c)$. Consequently, all terms in Eq. (10) are $\mathcal{O}(N_c)$. The color traces of eq.10 can be evaluated [16]

$$\begin{aligned} & \text{tr}_c \log \left(1 + L e^{-(E_i - \mu_i)/T} \right) = \\ & \log \left[1 + 3(\Phi + \bar{\Phi} e^{-(E_i - \mu_i)/T}) e^{-(E_i - \mu_i)/T} \right. \\ & \left. + e^{-3(E_i - \mu_i)/T} \right], \quad (11) \end{aligned}$$

$$\begin{aligned} & \text{tr}_c \log \left(1 + L^\dagger e^{-(E_i + \mu_i)/T} \right) = \\ & \log \left[1 + 3(\bar{\Phi} + \Phi e^{-(E_i + \mu_i)/T}) e^{-(E_i + \mu_i)/T} \right. \\ & \left. + e^{-3(E_i + \mu_i)/T} \right]. \quad (12) \end{aligned}$$

To obtain the expectation values of the chiral condensate $\langle \bar{\psi}_i \psi_i \rangle$ and the homogeneous Polyakov loop fields $\langle \Phi \rangle$ and $\langle \bar{\Phi} \rangle$, one has to minimize Ω with respect to these variables.

$$\begin{aligned} & \frac{\partial \Omega_{PNJL}}{\partial \phi} = 0 \\ & \frac{\partial \Omega_{PNJL}}{\partial \bar{\phi}} = 0 \\ & \frac{\partial \Omega_{PNJL}}{\partial \langle \bar{\psi} \psi \rangle_q} = 0 \\ & \frac{\partial \Omega_{PNJL}}{\partial \langle \bar{\psi} \psi \rangle_s} = 0. \quad (13) \end{aligned}$$

The indices d and s stand for up/down quarks and strange quarks, respectively. The minimizing with respect to the condensates can be replaced by a minimizing with respect to the masses. It leads to the well known NJL gap equations [16, 21, 27]:

$$m_i = m_{i0} - 4G\langle\bar{\psi}_i\psi_i\rangle + 2H\langle\bar{\psi}_j\psi_j\rangle\langle\bar{\psi}_k\psi_k\rangle, \quad j, k \neq i; j \neq k. \quad (14)$$

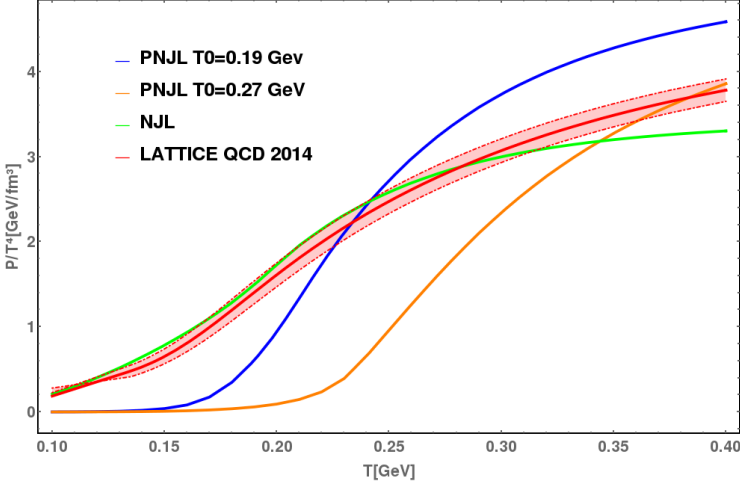


FIG. 1. Comparison of the pressure from IQCD [30], NJL and PNJL calculations. In PNJL we use two values of T_0 : 270 MeV (pure Yang Mills) and 190 MeV to account for the interactions between gluons and quarks [31].

The pressure is obtained by subtracting from $-\Omega$ the vacuum pressure (taken numerically at $T = 0.001 \text{ GeV}$ and $\mu = 0 \text{ GeV}$):

$$P = -\Omega(T, \mu) - \Omega(0.001, 0). \quad (15)$$

The pressure obtained in the NJL model, in two different parametrisations of the PNJL model and from the lattice calculations is shown in fig. 1. The NJL model seems to be close to the lattice results, especially at low temperature, but this is an artifact of the model. At low temperature quarks are confined and the pressure is created from hadrons. There the Hadron Resonance Gas theory matches very well with lattice results. The lack of confinement in the NJL model leads at low T, however, to a non vanishing pressure of the quarks. The PNJL model has also no confinement but suppresses quark degrees of freedom at temperatures below the critical temperature. The pressure drops quickly with decreasing T as a consequence of the statistical confinement induced by the coupling with the Polyakov loop. At high temperature, NJL does not saturate at the same pressure as the lattice calculations because of the lack of gluons whose contribution to the pressure is missed. The PNJL model with $T_0 = 270 \text{ MeV}$, corresponding to a pure Yang Mills medium, has a vanishing pressure at low temperature because of the statistical confinement but does not match the IQCD pressure either above the critical temperature as the gluon contribution do not involve quark-gluons interaction. The PNJL calculations for $T_0 = 190 \text{ MeV}$ [31], which take into consideration the presence of quarks in the medium in an approximate

way, has the same features than that for $T_0 = 270 \text{ MeV}$ but saturate more closely to the lattice results around the critical temperature. However, the phase transition remains too sharp to match them.

As a consequence, the reproduction of lattice results requires the addition of a mesonic pressure at low temperature vanishing naturally at high temperature and a more evolved description of the quark-gluon interaction which we will obtain using a phenomenological parametrisation of the T_0 parameter of the PNJL model.

III. THE GRAND-CANONICAL POTENTIAL IN $\mathcal{O}(N_c = 0)$

The next to leading order in N_C of the grand-canonical potential adds in a natural way the pressure of mesons below T_C . The details of the calculation of the grand-canonical potential in order $\mathcal{O}(N_c = 0)$, $\Omega_q^{(0)}$, have been discussed in ref.[16]. Therefore we mention here only the results which are necessary for the understanding of this paper. In next to leading order the quark grand-canonical potential, $\Omega_q^{(0)}$, becomes a function of the mesons, or, more precisely, of the quark-antiquark correlation function $\Pi(\omega, \mathbf{p})$

$$\Omega_q^{(0)}(T, \mu_i) = \sum_{M \in J^\pi = \{0^+, 0^-\}} \Omega_M^{(0)}(T, \mu_M(\mu_i)), \quad (16)$$

where M denotes the contribution of the scalar and pseudoscalar, $J^\pi = \{0^+, 0^-\}$, mesons. $\Omega^{(0)}$ can be expressed as

$$\begin{aligned} \Omega_M^{(0)}(T, \mu_M) &= \frac{g_M}{2} \int \frac{d^3p}{(2\pi)^3} \frac{1}{2\pi i} \int_0^{+\infty} d\omega \\ &\left[1 + \frac{1}{e^{\beta(\omega - \mu_M)} - 1} + \frac{1}{e^{\beta(\omega + \mu_M)} - 1} \right] \\ &\times \log \frac{1 - 2\mathcal{K}_M \Pi(\omega - \mu_M + i\epsilon, \mathbf{p})}{1 - 2\mathcal{K}_M \Pi(\omega - \mu_M - i\epsilon, \mathbf{p})}. \end{aligned} \quad (17)$$

and is a function of the quark-antiquark correlation function

$$\begin{aligned} i\Pi_{qq'}^M(i\omega_m, \mathbf{p}) &= -iT \sum_n \int \frac{d^3k}{(2\pi)^3} \\ &\cdot \text{Tr} [\bar{\Omega}_q S_q(i\nu_n, \mathbf{k}) \Omega_{q'} S_{q'}(i\nu_n - i\omega_m, \mathbf{k} - \mathbf{p})], \end{aligned} \quad (18)$$

where $S_q(i\nu_n, \mathbf{k})$ is the propagator of a quark of flavor q in the Hartree approximation. The trace is to be taken in color, flavor and spin spaces ($\text{Tr} = \text{tr}_c \text{tr}_f \text{tr}_\gamma$). The factor Ω_q is

$$\Omega_q = \mathbb{I}_c \otimes \tau^a \otimes \Gamma_M, \quad (19)$$

where \mathbb{I}_c is the unit matrix in color space and $\Gamma_M = \{\mathbb{I}, i\gamma_5\}$ for scalar and pseudoscalar channels, respectively. The same quark-antiquark propagator $\Pi(\omega, \mathbf{p})$ appears in the determination of the meson mass and

width. Exploiting the Jost representation of the scattering amplitude one can obtain in the no-sea approximation (means by neglecting the first term in the brackets of eq. 17) an alternative form

$$\Omega_M^{(0)}(T, \mu_M) = -\frac{g_M}{2\pi} \int \frac{d^3p}{(2\pi)^3} \int_0^{+\infty} d\omega \left[\frac{1}{e^{\beta(\omega - \mu_M)} - 1} + \frac{1}{e^{\beta(\omega + \mu_M)} - 1} \right] \delta(\omega, \mathbf{p}; T, \mu_M), \quad (20)$$

with

$$\begin{aligned} \delta_M(\omega, \mathbf{p}; T, \mu_M) &= -\frac{1}{2i} \log \frac{1 - 2\mathcal{K}_M \Pi_M(\omega - \mu_M + i\epsilon, \mathbf{p})}{[1 - 2\mathcal{K}_M \Pi_M(\omega - \mu_M + i\epsilon, \mathbf{p})]^*} \\ &= -\frac{1}{2i} \log |1| - \frac{1}{2} \text{Arg} \frac{1 - 2\mathcal{K}_M \Pi_M(\omega - \mu_M + i\epsilon, \mathbf{p})}{[1 - 2\mathcal{K}_M \Pi_M(\omega - \mu_M + i\epsilon, \mathbf{p})]^*} \\ &= -\text{Arg} [1 - 2\mathcal{K}_M \Pi_M(\omega - \mu_M + i\epsilon, \mathbf{p})]. \end{aligned} \quad (21)$$

A simplifying assumption has been proposed in [32, 33] to make the argument of the phase shifts approximately Lorentz invariant. One introduces the Mandelstam variable $s = \omega^2 - p^2$, and assumes that

$$\begin{aligned} \delta_M(\omega, \mathbf{p}; T, \mu_M) &\simeq \delta_M(\sqrt{\omega^2 - \mathbf{p}^2}, \mathbf{p} = \mathbf{0}; T, \mu_M) \\ &= \delta_M(\sqrt{s}, \mathbf{p} = \mathbf{0}; T, \mu_M). \end{aligned} \quad (22)$$

With this approximation we obtain for the meson part of the grand-canonical potential

$$\begin{aligned} \Omega_M^{(0)}(T, \mu_M) &= -\frac{g_M}{8\pi^3} \int dp p^2 \int \frac{ds}{\sqrt{s + p^2}} \\ &\left[\frac{1}{e^{\beta(\sqrt{s+p^2} - \mu_M)} - 1} + \frac{1}{e^{\beta(\sqrt{s+p^2} + \mu_M)} - 1} \right] \\ &\quad \times \delta_M(\sqrt{s}; T, \mu_M), \end{aligned} \quad (23)$$

where the phase shift is computed using Eq. (21).

A. Interaction between quarks and gluons

The interaction of quarks and gluons, represented by the Polyakov loop field, modifies not only the quark properties but the gluon field itself. This back reaction has been studied in ref.[31] by comparing the pure Yang Mills potential U_{YM} with U_{glue} obtained, when allowing for quark-antiquark excitation in the gluon propagator. The authors found that the quark-antiquark loops change U_{YM} considerably. U_{glue} is related to U_{YM} by

$$\frac{\mathcal{U}_{glue}}{T^4}(t_{glue}, \Phi, \bar{\Phi}) = \frac{\mathcal{U}_{YM}}{T^4}(t_{YM}(t_{glue}), \Phi, \bar{\Phi}), \quad (24)$$

where t is the reduced temperature. t_{YM} and t_{glue} are related by:

$$t_{YM} = \frac{T - T_{YM}^{cr}}{T_{YM}^{cr}} = 0.57 \frac{T - T_{glue}^{cr}}{T_{glue}^{cr}} = 0.57 t_{glue}. \quad (25)$$

T_{YM}^{cr} is the deconfinement temperature in the pure YM case (and fixed to $T_{YM}^{cr} = 270$ MeV), whereas T_{glue}^{cr} is the transition temperature in the unquenched case. The numerical coefficient 0.57 is the outcome from the comparison of the two effective potentials. This procedure

rescales the critical temperature from $T_{YM}^{cr} = 270$ MeV to $T_{glue}^{cr} = 190$ MeV.

In this article we go beyond a pure rescaling of the temperature due to the presence of the quarks and modify the parameters of the U_{glue} by:

$$\frac{U(\phi, \bar{\phi},)}{T^4} = -\frac{b_2(T)}{2} \bar{\phi}\phi - \frac{b_3}{6} (\bar{\phi}^3 + \phi^3) + \frac{b_4}{4} (\bar{\phi}\phi)^2 \quad (26)$$

with the parameters : $b_2(T) = a_0 + \frac{a_1}{1+\tau} + \frac{a_2}{(1+\tau)^2} + \frac{a_3}{(1+\tau)^3}$ where:

$$\tau_{phen} = 0.57 \frac{T - T_{phen}^{cr}(T)}{T_{phen}^{cr}(T)}. \quad (27)$$

We assume a phenomenological temperature dependence of T_{phen}^{cr} of the form

$$T_{phen}^{cr}(T) = a + bT + cT^2 + dT^3 + e\frac{1}{T}. \quad (28)$$

and determine the coefficients a,...,e, see table II, by comparison with lattice gauge calculations.

a_0	a_1	a_2	a_3	b_3	b_4	a	b	c	d	e
6.75	-1.95	2.625	-7.44	0.75	7.5	0.082	0.36	0.72	-1.6	-0.0002

TABLE II. Full table of parameters for the PNJL model

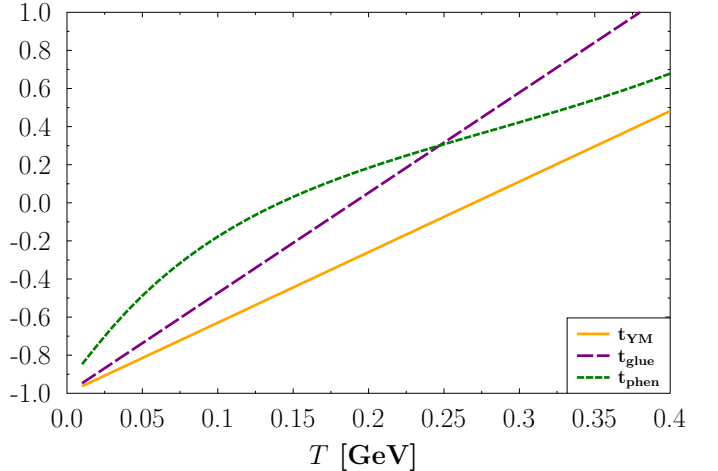


FIG. 2. t_{YM} , t_{glue} [31] and t_{phen} as function of the temperature

This new parametrisation leaves the asymptotic limit of the gluon pressure unchanged. The rescaling is now a function of the temperature assuming that the quark-antiquark excitation depend on the temperature of the

medium. The parametrisation is taken to be polynomial. The term in T^{-1} does not depend on the quark-gluon interaction. It increases the pressure at low temperature and compensates partially for the fact that only four types of mesons (π , K , σ , a_0) are taken into consideration at the moment. In Fig. 2 we compare the different reduced temperatures for pure Yang-Mills, from [31] Eq. 25 and from our approach Eq. 27. We see that our reduced temperature t_{phen} is higher at low temperature (where hadrons are the relevant degrees of freedom) but comes close to the effective temperature of [31] around the phase transition temperature. It tends to the pure Yang Mills reduced temperature for high temperatures, as it should, because asymptotically we expect a plasma of noninteracting quarks and gluons.

IV. RESULTS

A. Equation of state at vanishing chemical potential

As we have seen in Fig. 1, the PNJL approach with a constant T_0 and $\mu = 0$ does not match the lattice equation of state.

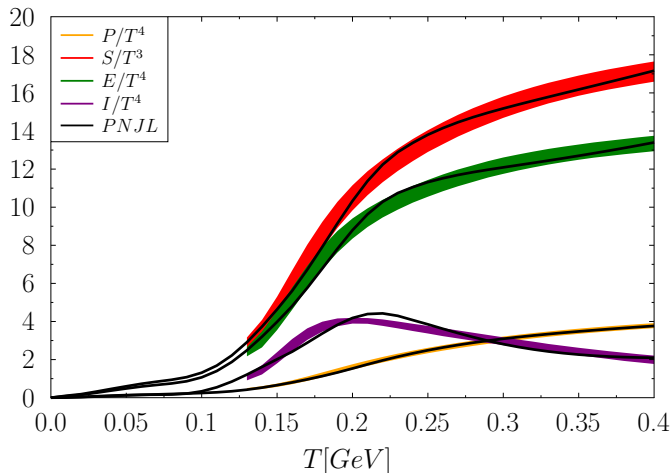


FIG. 3. Pressure, entropy density, energy density and interaction measure calculated with PNJL, using eq. 28, for $\mu = 0$. We compare our results (lines) with the lattice results (colored areas) [3]

Using the temperature dependent interaction between quarks and gluons with the parametrisation given above and taking into consideration the contribution of pseudoscalar pions and kaons and scalar mesons, σ and a_0 , which contribute to the next to leading order terms of the partition sum, we can reproduce the pressure as function of the temperature obtained by lattice gauge calculations [30]. This is shown in Fig. 3. On the

hadronic side of the phase diagram, we expect that also higher mass hadrons contribute to the pressure even if their larger mass suppresses their contribution. Also the derivatives of the pressure as entropy, energy density and interaction measure reproduce well the results of lattice gauge calculations.

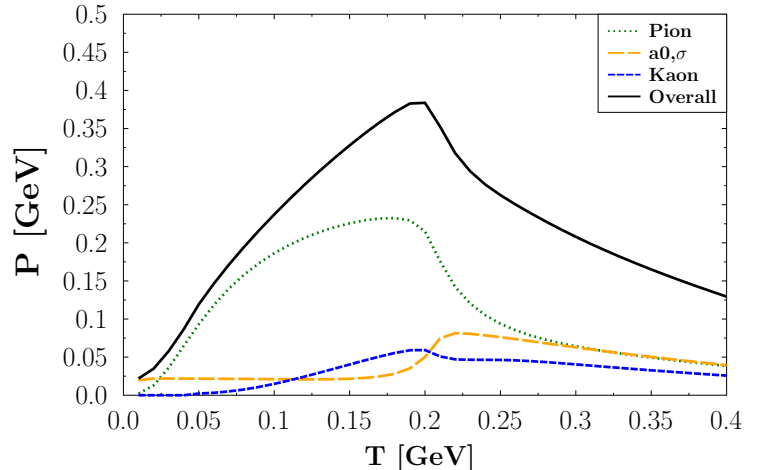


FIG. 4. Different mesonic contributions to the pressure at $\mu = 0$

Fig. 4 shows the contribution to the pressure of the different mesons included in our calculation. In leading order in N_c neither in NJL nor in PNJL such a contribution exists. Being the lightest meson, the pseudoscalar pion is contributing most to the pressure. Although unstable, the mesons contribute to the pressure also above the phase transition but naturally this contribution tends to vanish at large temperatures. The pressure of the scalar mesons exhibits two different contributions. Due to its large width the scalar σ contributes to the pressure already at very low temperatures. At higher temperatures, we observe a chiral restoration for the scalar and pseudoscalar mesons which have there the same finite mass and consequently the same contribution to the pressure.

In Fig. 5 we show the pressure contribution of gluons, quarks and mesons as a function of the temperature. At high temperatures, the pressure is dominated by the quark contribution. Mesons dominate at low temperature and present a non negligible contribution around T_c indicating that at $\mu = 0$ we have a cross over and not a sharp transition between the phases. The gluon pressure is negative at low temperature what can be interpreted as an attractive interaction. It becomes positive at higher temperature and reaches asymptotically the YM pressure.

Another quantity of interest is the speed of sound which is related to the compressibility of the system.

$$c_s^2 = \frac{\partial P}{\partial \epsilon} = \frac{\partial P}{\partial T} / \frac{\partial \epsilon}{\partial T} \Big|_{\mu=0}. \quad (29)$$

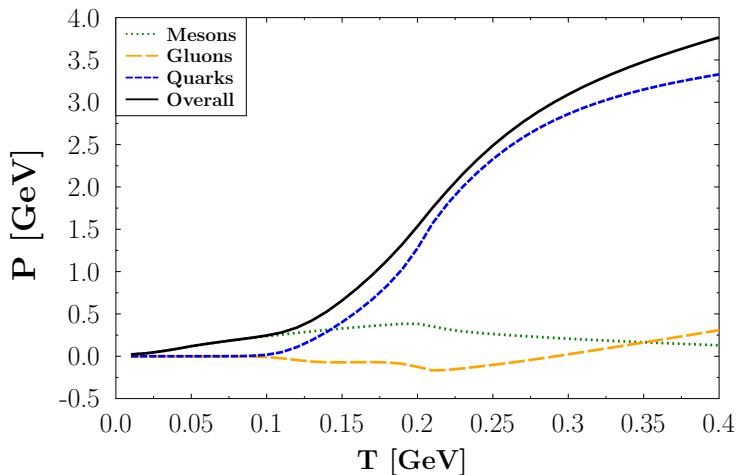


FIG. 5. The different contributions to the total pressure at $\mu = 0$ as a function of the temperature.

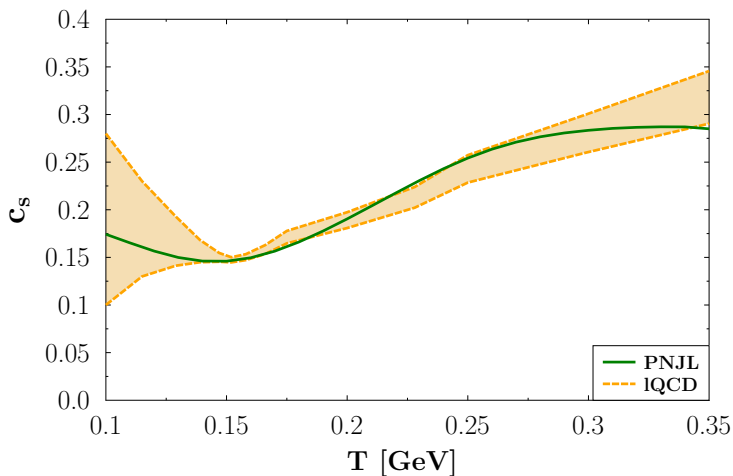


FIG. 6. Speed of sound at $\mu = 0$. We compare lattice calculations [34] with our approach.

Lattice calculations have found that the softest point of the equation of state, the minimum of the speed of sound is slightly below the cross over temperature [34]. In our PNJL calculation we obtain a shallow minimum which is close to the value obtained from the lattice gauge calculations. The fact that not all hadrons of the hadronic spectrum are included in our calculation leads to a slightly enhanced b coefficient in the effective parametrisation of the T_0 temperature Eq. 28. As a consequence the speed of sound increase is less pronounced below T_c and the minimum gets shallower. We expect that the inclusion of more hadrons will localize the minimum more precisely. As we will see below this would help to determine the critical temperature T_c

more precisely.

B. Taylor expansion around $\mu = 0$

In the (P)NJL approach the extension to a finite chemical potential is straight forward. One has only to add a chemical potential in the distribution function of the quarks. We can therefore, without introducing any new parameter, calculate the thermodynamical quantities in the whole μ, T plane. To make contact with the lattice gauge calculations we can, however, also apply the same procedure by which in lattice gauge calculations the thermodynamical quantities are calculated for small but finite μ . For this we apply a Taylor expansion of the critical temperature around zero baryonic potential:

$$\frac{T_c(\mu_B)}{T_c(0)} = 1 - \kappa \left(\frac{\mu_B}{T_c(\mu_B)} \right)^2 + \dots \quad (30)$$

The κ coefficient is [36]:

$$\kappa = -T_c(0) \left. \frac{\partial T_c(\mu_B)}{\partial (\mu_B)^2} \right|_{\mu_B=0} \quad (31)$$

At $\mu_B = 0$, we get the critical temperature, determined as the minimum of the speed of sound (see Fig. 6), :

$$T_c = 146 \text{ MeV} \quad (32)$$

The corresponding κ coefficient is :

$$\kappa = 0.01. \quad (33)$$

In Fig. 7 this coefficient is compared with the result of lattice calculations and is found to be in good agreement. Consequently, our PNJL approach agrees with lattice data also for finite but small chemical potentials.

C. Calculation at finite μ

After having verified that our approach agrees with lattice calculation for small μ we investigate the large μ limit of our approach. Then one can compare our results with perturbative QCD calculations in the hard dense loop formalism ref.[14]. As seen in Fig.8 our approach agrees also in this limit quite well with QCD calculations.

Having verified that our PNJL approach gives the right value of the pressure for a vanishing and for large chemical potentials we have a solid basis to study the phase diagram in between the two extremes. The result

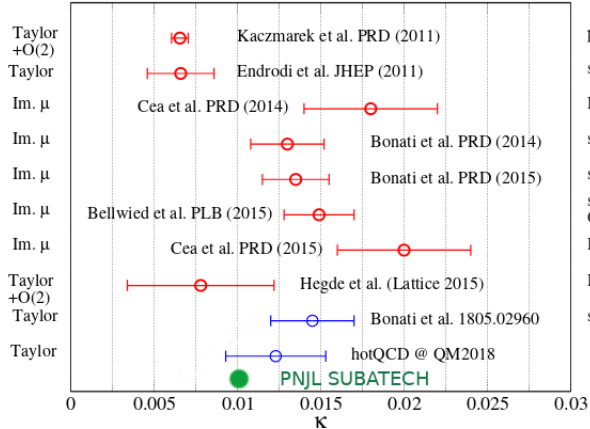


FIG. 7. The expansion coefficient of the first order Taylor expansion for finite μ in different approaches.

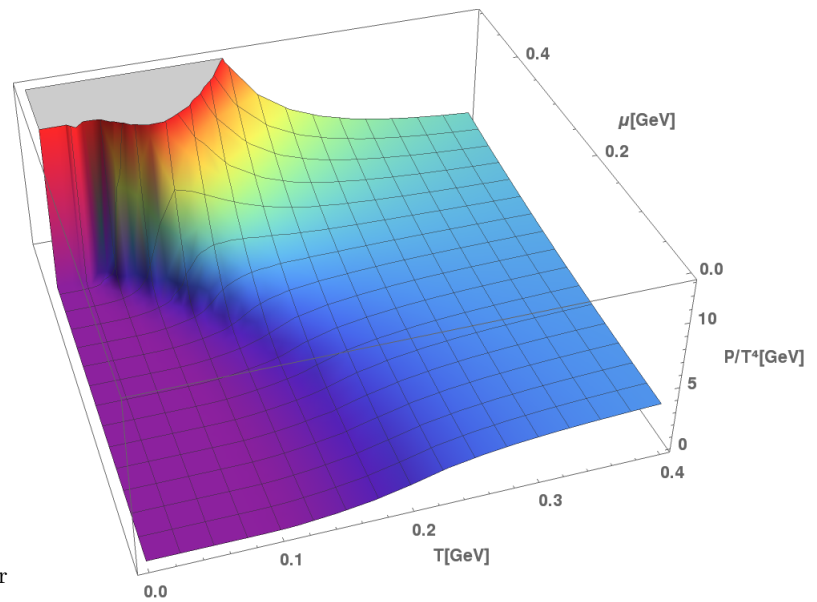


FIG. 9. P/T^4 as a function of T and μ

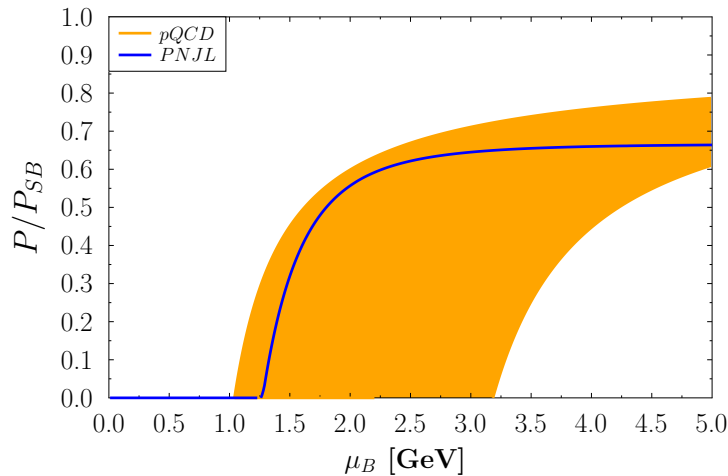


FIG. 8. The quark pressure as a function of μ for a temperature of $T = 0.001$ GeV. We compare pQMD calculations [14] (orange area) with the result of our pQMD approach (blue line).

of our calculation is presented in Fig. 9. We see that the cross over between hadronic and quark phase continues for finite values of μ , as predicted by the lattice results. With increasing chemical potential the cross over becomes steeper and steeper and finally ends up in a first order phase transition. The increase of the pressure at high μ is dominated by the $\frac{1}{T^4}$ factor in $\frac{P}{T^4}$.

D. Phase Transition

We study now the structure of this phase transition. For very low temperatures, the phase diagram is char-

acterized by a first order phase transition at a critical quark chemical potential of $\mu_c = 0.425$ GeV. The order parameter of this phase transition is the quark mass. Its dependence on the quark chemical potential is displayed in Fig. 10 (for a temperature of $T = 0.001$ GeV). We see clearly the shape of a first order phase transition. Although the critical chemical potential can be determined by a Maxwell construction it is preferable to use the Grand Potential as a function of μ_q which is displayed in Fig. 11. We see there a crossing of two phases: the phase where the mass of the quarks is close to their bare mass (orange line) and in which the chiral symmetry is restored, and a phase where the quark masses are dressed because of the interactions with the medium (green line). Below the critical chemical potential μ_c hadrons are the thermodynamically relevant degrees of freedom, above μ_c this role is played by the quarks. The crossing point determines the critical chemical potential $\mu_c(T) = 0.425$ GeV.

Fig. 12 shows the pion mass and the sum of up and down quark mass as a function of μ_q . The mass of the pion, being a Goldstone boson, remains constant up to $\mu_q \approx 0.42$ GeV and increases moderately for larger μ_q . At the phase transition the pion mass becomes larger than the sum of the quark masses and quarks get the relevant degrees of freedom.

μ_c decreases as a function of the temperature and finally the transition becomes a cross over. The cross over region and the first order region are separated by the critical end point, CEP. The gap equations 14 provides the most convenient way to calculate the critical end point. The CEP is reached when the first and second derivative of the mass with respect to the chemical potential becomes infinite.

To simplify the system, we express everything in terms of the gap equations and we obtain a system of six

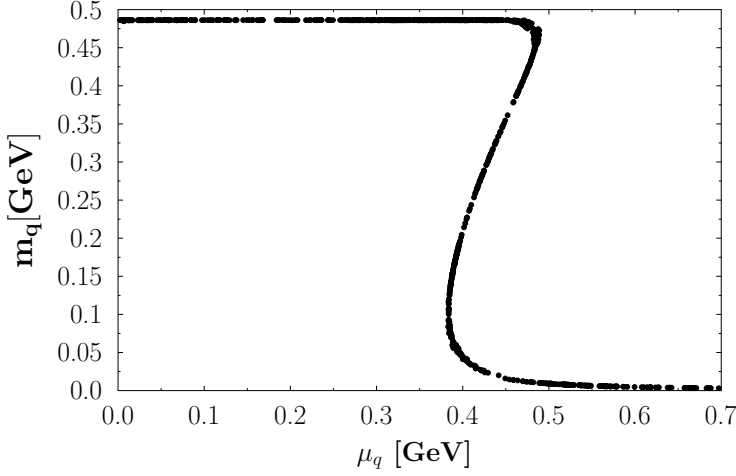


FIG. 10. Mass of the u quark around the quark chemical potential for which a first order chiral phase transition occurs for a temperature of $T = 0.001 \text{ GeV}$.

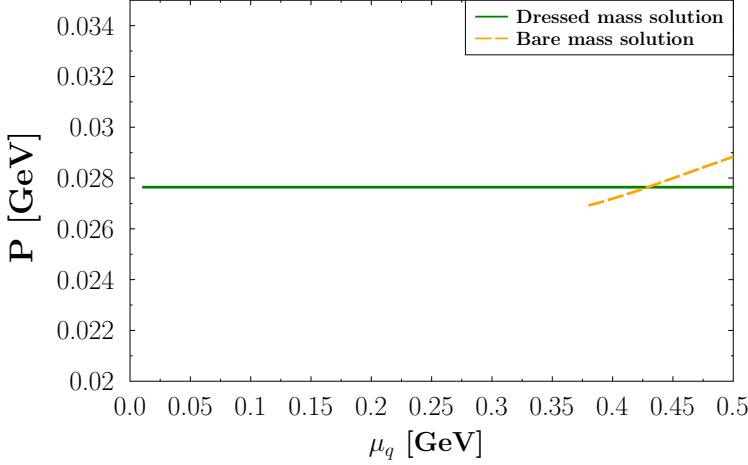


FIG. 11. Pressure obtain from the dressed mass (green line) sand bare mass (orange line) solutions to equation 13.

equations with six unknowns: the masses of the u and s quarks, the Polyakov loop ϕ and its complex conjugate $\bar{\phi}$, the temperature and the chemical potential ref.[35]:

$$\begin{aligned}
 g_u(\mu, T, mq, ms, \phi, \bar{\phi}) &= 0 \\
 \frac{\partial \Omega_{PNJL}(\mu, T, mq, ms, \phi, \bar{\phi})}{\partial \phi} &= 0 \\
 \frac{\partial \Omega_{PNJL}(\mu, T, mq, ms, \phi, \bar{\phi})}{\partial \bar{\phi}} &= 0 \\
 g_s(\mu, T, mq, ms, \phi, \bar{\phi}) &= 0 \\
 \frac{\frac{\partial g_u(\mu, T, mq, ms, \phi, \bar{\phi})}{\partial mq}}{\frac{\partial g_u(\mu, T, mq, ms, \phi, \bar{\phi})}{\partial \mu}} &= 0 \\
 \frac{\frac{\partial^2 g_u(\mu, T, mq, ms, \phi, \bar{\phi})}{\partial mq^2}}{\frac{\partial g_u(\mu, T, mq, ms, \phi, \bar{\phi})}{\partial \mu}} &= 0
 \end{aligned} \tag{34}$$

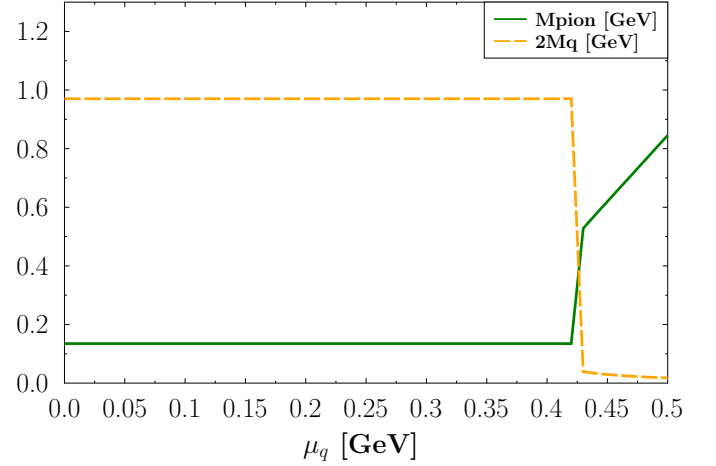


FIG. 12. Meson and quark masses at vanishing temperature.

The solution of this system is $T_{CEP} = 0.11 \text{ GeV}$ and $\mu_{CEP} = 0.32 \text{ GeV}$.

Fig. 13 displays the relevant temperatures, as a function of the chemical potential, of our calculations. We show the Mott temperature of kaons and pions. This is the temperature at which the sum of the masses of the constituent quarks equals the mass of the meson. This temperature is a decreasing function of the temperature and very similar for kaons and pions.

The temperature of the minimum of the speed of sound is always well below the Mott temperature and (as the lattice calculations for $\mu = 0$) below the transition temperature determined by the inflection point of the lattice as a function of the temperature.

Can this chiral phase transition be studied by heavy ion experiments? To discuss this question we compare in Fig. 14 in the T, μ plane the line of the chiral first order phase transition with the freeze out curve, calculated by Cleymans and al. [6], which is determined by fitting

V. CONCLUSION

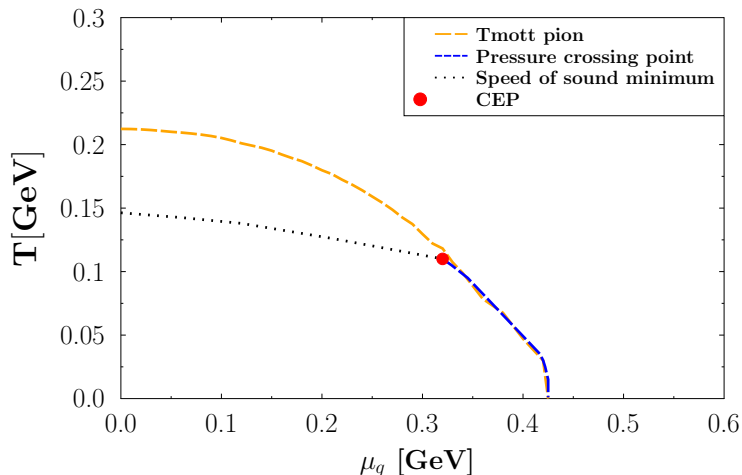


FIG. 13. Phase diagram of strongly interacting matter described by our PNJL approach.

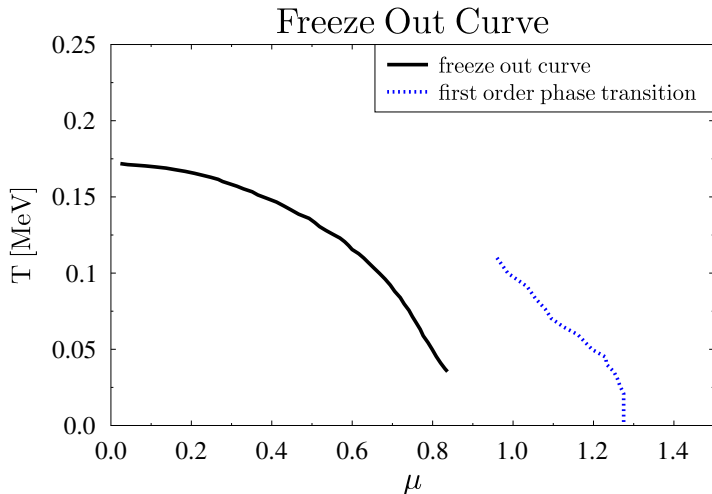


FIG. 14. Freeze-out curve from statistical model calculations [6].

the observed hadron multiplicities in the framework of a statistical model. In this approach it is assumed that after having passed the freeze-out line hadrons scatter only elastically. The point in the T, μ plane which is reached in heavy ion collisions before the system expands is not known and even whether the system comes to thermal equilibrium before the freeze-out is debated. To be consistent it has to be above the freeze-out curve. Our PNJL approach fulfills this condition and the distance between the freeze-out line and the line of the first order phase transition is small. Therefore to study this first order chiral phase transition may be in reach in heavy-ion experiments.

This work presents an improved version of the PNJL model. As compared to the standard version we have added the next to leading order (in N_c) contribution to the partition function. In this order we obtain contributions from mesons and therefore the description of the thermodynamical properties below the transition temperature is largely improved. We modified also the phenomenological parametrization of the interaction between quarks and gluons which goes beyond a simple rescaling of the critical temperature T_0 . Calculating the thermodynamical properties of the system we could show that for vanishing chemical potential we reproduce the results for pressure, energy density, entropy density and interaction measure from lattice gauge calculations. Also the speed of sound agrees within the error bars with the prediction from lattice calculations.

For a small but finite chemical potential our approach reproduces lattice results as well. We showed that the expansion coefficient in μ/T is in between the error bars of recent lattice calculations.

The (P)NJL calculations can be extended without any new parameter to large chemical potentials. For very large chemical potentials we compared the pressure with pQCD calculations and find agreement. Having verified that at small (vanishing) chemical potentials as well as at very large chemical potentials our PNJL approach agrees with less phenomenological approaches we can investigate the whole T, μ phase diagram. Our calculations predict a first order phase transition with a critical end point of $T_{CEP} = 110$ MeV and $\mu_q = 320$ MeV. Comparing our results with the chemical freeze out curve of statistical model calculations it seems to be possible that the first order phase transition can be investigated in heavy ion reactions at beam energies in the region between 3 and 10 AGeV. Heavy ions with these energies will become available soon at the new facilities under construction.

This work opens as well the perspective to explore in the finite μ region heavy ion reactions theoretically by hydrodynamical models, where the equation of state is an input, or by dynamical models, whose parameters can be calibrated to the equation of state like the dynamical quasi-particle model. Even more, the line of the first order phase transition in the T, μ plane and the freeze-out line, where, based on statistical model calculations, inelastic collisions cease, are not distant, so it may be possible to study even the first order phase transition line in heavy-ion experiments.

This work allows also to study neutron star physics and collisions among neutron stars, both phenomena in which the equation of state plays an essential role. This will be the subject of an upcoming publication.

VI. ACKNOWLEDGMENT

We would like to thank A. Vuorinen for providing the code to compare our results with the large μ pQCD limit and for his advice as well as F. Mathieu, L. Pied, F. Cougoulic, G.Sophys, S.Delorme and M. Pierre for valuable discussions. We acknowledge funding by the Region Pays de la Loire and by the CNRS-IN2P3.

-
- [1] S. Bose, K. Chakravarti, L. Rezzolla, B. S. Sathyaprakash and K. Takami, Phys. Rev. Lett. **120** (2018) no.3, 031102.
- [2] S. Borsanyi, Z. Fodor, C. Hoelbling, S. D. Katz, S. Krieg and K. K. Szabo, Phys. Lett. B **730**, 99 (2014).
- [3] A. Bazavov *et al.* [HotQCD Collaboration], Phys. Rev. D **90**, 094503 (2014).
- [4] P. Braun-Munzinger, V. Koch, T. Schfer and J. Stachel, Phys. Rept. **621** (2016) 76.
- [5] J. Stachel, A. Andronic, P. Braun-Munzinger and K. Redlich, J. Phys. Conf. Ser. **509** (2014) 012019.
- [6] J. Cleymans, H. Oeschler, K. Redlich and S. Wheaton, Phys. Rev. C **73** (2006) 034905.
- [7] C. Gale, S. Jeon and B. Schenke, Int. J. Mod. Phys. A **28** (2013) 1340011.
- [8] M. Bluhm, P. Alba, W. Alberico, R. Bellwied, V. Mantovani Sarti, M. Nahrgang and C. Ratti, Nucl. Phys. A **931** (2014) 814.
- [9] A. Bazavov *et al.*, Phys. Rev. D **95** (2017) no.5, 054504.
- [10] J. N. Guenther, R. Bellwied, S. Borsanyi, Z. Fodor, S. D. Katz, A. Pasztor, C. Ratti and K. K. Szab, Nucl. Phys. A **967** (2017) 720.
- [11] M. Asakawa and K. Yazaki, Nucl. Phys. A **504** (1989) 668.
- [12] M. A. Stephanov, K. Rajagopal and E. V. Shuryak, Phys. Rev. Lett. **81** (1998) 4816
- [13] M. A. Stephanov, K. Rajagopal and E. V. Shuryak, Phys. Rev. D **60** (1999) 114028
- [14] A. Kurkela and A. Vuorinen, Phys. Rev. Lett. **117** (2016) no.4, 042501
- [15] A. Vuorinen, EPJ Web Conf. **137** (2017) 09011
- [16] J. M. Torres-Rincon and J. Aichelin, Phys. Rev. C **96** (2017) no.4, 045205.
- [17] J. M. Torres-Rincon and J. Aichelin, arXiv:1601.01706 [nucl-th].
- [18] K. Fukushima, Phys. Lett. B **591** (2004) 277.
- [19] E. Megias, E. Ruiz Arriola and L. L. Salcedo, Phys. Rev. D **74** (2006) 065005.
- [20] C. Ratti, M. A. Thaler and W. Weise, Phys. Rev. D **73** (2006) 014019.
- [21] H. Hansen, W. M. Alberico, A. Beraudo, A. Molinari, M. Nardi and C. Ratti, Phys. Rev. D **75** (2007) 065004.
- [22] Y. Nambu and G. Jona-Lasinio, Phys. Rev. **124** (1961) 246.
- [23] I. C. Cloet and C. D. Roberts, Prog. Part. Nucl. Phys. **77** (2014) 1.
- [24] J. M. Torres-Rincon, B. Sintes and J. Aichelin, Phys. Rev. C **91** (2015) no.6, 065206.
- [25] U. Vogl and W. Weise, Prog. Part. Nucl. Phys. **27** (1991) 195.
- [26] S. P. Klevansky, Rev. Mod. Phys. **64** (1992) 649.
- [27] M. Buballa, Phys. Rept. **407** (2005) 205.
- [28] C. R. Allton, S. Ejiri, S. J. Hands, O. Kaczmarek, F. Karsch, E. Laermann and C. Schmidt, Phys. Rev. D **68** (2003) 014507.
- [29] M. Cheng *et al.*, Phys. Rev. D **81** (2010) 054504.
- [30] A. Bazavov, Tanmoy Bhattacharya, C. DeTar, H. -T. Ding, Steven Gottlieb, Rajan Gupta, P. Hegde, U. M. Heller, F. Karsch, E. Laermann, L. Levkova, Swagato Mukherjee, P. Petreczky, C. Schmidt, C. Schroeder, R. A. Soltz, W. Soeldner, R. Sugar, M. Wagner and P. Vrana, arXiv:1407.6387, 2014.
- [31] L. M. Haas, R. Stiele, J. Braun, J. M. Pawlowski and J. Schaffner-Bielich, Phys. Rev. D **87**, no. 7, 076004 (2013).
- [32] J. Hufner, S. P. Klevansky, P. Zhuang and H. Voss, Annals Phys. **234** (1994) 225.
- [33] D. Blaschke, M. Buballa, A. Dubinin, G. Roepke and D. Zablocki, Annals Phys. **348** (2014) 228
- [34] S. Borsanyi, G. Endrodi, Z. Fodor, A. Jakovac, S. D. Katz, S. Krieg, C. Ratti and K. K. Szabo, JHEP **1011** (2010) 077
- [35] A. Biguet, Modeles Nambu-Jona-Lasinio pour l'etude des phases de la chromodynamique quantique - qualites des predictions et phases hautes densites, univeristy of Lyon, 2016, <https://tel.archives-ouvertes.fr/tel-01453184/document>.
- [36] Claudio Bonati, Massimo D'Elia, Francesco Negro, Francesco Sanfilippo and Kevin Zambello, Phys. Rev. D **98**, 054510 (2018);